Monthly Notices of the ROYAL ASTRONOMICAL SOCIETY

MNRAS **525,** 415–427 (2023) https://doi.org/10.1093/mnras/stad2300
Advance Access publication 2023 August 28

Environmental effects on associations of dwarf galaxies

C. Yamila Yaryura,[1,2]★ Mario G. Abadi,[1,2]★ Stefan Gottlöber,[3] Noam I. Libeskind,[3,4] Sofía A. Cora,[5,6] Andrés N. Ruiz,[1,2] Cristian A. Vega-Martínez[7,8] and Gustavo Yepes[9,10]

[1]*CONICET-Universidad Nacional de Córdoba, Instituto de Astronomía Teórica y Experimental (IATE), Laprida 854, X5000BGR, Córdoba, Argentina*
[2]*Observatorio Astronómico, Universidad Nacional de Córdoba, Laprida 854, X5000BGR, Córdoba, Argentina*
[3]*Leibniz-Institut für Astrophysik Potsdam (AIP), An der Sternwarte 16, D-14482, Potsdam, Germany*
[4]*University of Lyon; Univ Claude Bernard Lyon 1, CNRS, IP2I Lyon / IN2P3, IMR 5822, F-69622, France*
[5]*Instituto de Astrofísica de La Plata (CCT La Plata, CONICET,UNLP), Observatorio Astronómico, Paseo del Bosque, 1900FWA, La Plata, Argentina*
[6]*Facultad de Ciencias Astronómicas y Geofísicas, Universidad Nacional de La Plata (UNLP), Observatorio Astronómico, Paseo del Bosque, B1900FWA La Plata, Argentina*
[7]*Instituto de Investigación Multidisciplinario en Ciencia y Tecnología, Universidad de La Serena, Raúl Bitrán 1305, La Serena, Chile*
[8]*Departamento de Astronomía, Universidad de La Serena, Av. Juan Cisternas 1200 Norte, La Serena, Chile*
[9]*Departamento de Física Teórica M-8, Universidad Autónoma de Madrid, Cantoblanco, E-28049 Madrid, Spain*
[10]*Centro de Investigación Avanzada en Física Fundamental (CIAFF), Universidad Autónoma de Madrid, E-28049 Madrid, Spain*

Accepted 2023 July 24. Received 2023 July 24; in original form 2022 October 4

ABSTRACT

We study the properties of associations of dwarf galaxies and their dependence on the environment. Associations of dwarf galaxies are extended systems composed exclusively of dwarf galaxies, considering as dwarf galaxies those galaxies less massive than $M_{\star,\max} = 10^{9.0}\ \mathrm{M}_{\odot}\ h^{-1}$. We identify these particular systems using a semi-analytical model of galaxy formation coupled to a dark matter-only simulation in the Λ Cold Dark Matter cosmological model. To classify the environment, we estimate eigenvalues from the tidal field of the dark matter particle distribution of the simulation. We find that the majority, two thirds, of associations are located in filaments (∼67 per cent), followed by walls (∼26 per cent), while only a small fraction of them are in knots (∼6 per cent) and voids (∼1 per cent). Associations located in more dense environments present significantly higher velocity dispersion than those located in less dense environments, evidencing that the environment plays a fundamental role in their dynamical properties. However, this connection between velocity dispersion and the environment depends exclusively on whether the systems are gravitational bound or unbound, given that it disappears when we consider associations of dwarf galaxies that are gravitationally bound. Although less than a dozen observationally detected associations of dwarf galaxies are currently known, our results are predictions on the eve of forthcoming large surveys of galaxies, which will enable these very particular systems to be identified and studied.

Key words: galaxies: dwarf – galaxies: groups: general – galaxies: kinematics and dynamics.

1 INTRODUCTION

The large-scale structure map of the Universe reveals that galaxy and dark matter (DM) distributions are not uniform, describing an intricate interconnected network known as the cosmic web. Within this network, galaxies, intergalactic gas, and DM are distributed within high-density regions as groups and clusters of galaxies, or along filaments and sheet-like walls, which surround very low-density regions known as voids. Most of the galaxies embedded in this cosmic web belong to systems that can contain from a few to hundreds even thousands of members (Huchra & Geller 1982; Yang et al. 2007; Tempel, Tago & Liivamägi 2012). These systems have been extensively studied and there is ample evidence that many of their observed properties are influenced by the web-like environment (Dressler 1980; Kauffmann et al. 2004; O'Mill, Padilla & García Lambas 2008; Peng et al. 2010; Zheng et al. 2017; Duplancic et al. 2020, among others). For example, it is known that elliptical galaxies are located more frequently in denser regions, while spiral galaxies are more common in the field (Dressler 1980). Similar trends are also detected for colours, star formation history, and the ages of galaxies (Blanton et al. 2005); in denser environments, there is a higher proportion of red and passive galaxies for a given stellar mass (Wetzel, Tinker & Conroy 2012; Wang et al. 2018). On the other hand, from a theoretical point of view, many studies show that the orientation of the haloes' minor axes shows a tendency to be perpendicular to the wall or filament where they reside. The spin orientation also correlates with the halo mass, being parallel to the filaments or walls for low-mass haloes and perpendicular for higher mass haloes (Aragón-Calvo et al. 2007; Hahn et al. 2007a, b; Zhang et al. 2009; Libeskind et al. 2013, among others).

Groups of galaxies are a particular type of system, being the most common structures of galaxies in the Universe. Even though there is no clear demarcation between groups and clusters, the latest

★ E-mail: yamila.yaryura@unc.edu.ar (CYY); mario.abadi@unc.edu.ar (MGA)

one are generally considered to contain hundreds or thousands of galaxies while groups contain only a few, with ∼50 being the most commonly used cut-off value when defining them. Their typical sizes are on average compared to a spherical volume of ∼ 1 Mpc of diameter. Their virial masses are, on average, approximately $\sim 10^{13}\,M_\odot\,h^{-1}$, and the velocity dispersion of their galaxy members are about ∼ 150 km s^{-1}. These groups can host very bright galaxies as well as fainter galaxies. However, the pioneering work of Tully (1987) revealed the existence of a very striking type of groups called *'associations of dwarf galaxies'*. These systems have the particularity of being extended systems, with typical sizes of $\sim 0.2\,\mathrm{Mpc}\,h^{-1}$, composed only of dwarf galaxies, extracted from the Nearby Galaxies Catalog (Tully 1988). They use a merging-tree algorithm to define these systems, where the luminosity density, determined by the combined luminosities and separations of contributing systems, was used to characterize the linkages between galaxies. Two levels of structure, namely 'groups' and 'associations' were defined based on luminosity density thresholds. We focus on *'associations of dwarf galaxies'* derived from linkages between galaxies that had insignificant luminosities, making the luminosity density fail to reach the threshold required to be classified as a group (see Tully 1987 for a exhaustive depiction of the method).

Among the very few works that study these particular systems, Tully et al. (2006) present a detailed description of the only seven associations of dwarf galaxies observed up to now and their main dynamical properties. Among these properties we can highlight their velocity dispersions covering a range between ∼20 and ∼ 75 km s^{-1}, their sizes around $0.2\,\mathrm{Mpc}\,h^{-1}$ and their virial masses ranging between $\sim 10^{10.5}$ and $\sim 10^{11.8}\,M_\odot\,h^{-1}$. From the theoretical point of view, Yaryura et al. (2020) present a study of associations of dwarf galaxies in the cosmological framework of the Λ Cold Dark Matter (ΛCDM) model, applying a semi-analytic model of galaxy formation to a DM-only *N*-body numerical simulation. They conclude that the ΛCDM model is able to reproduce these particular systems. On average, these simulated systems have typical sizes of $\sim 0.2\,\mathrm{Mpc}\,h^{-1}$, velocity dispersions of ∼ 30 km s^{-1} and estimated total masses of $\sim 10^{11}\,M_\odot\,h^{-1}$. These main dynamical properties mean values are comparable to the observational results presented by Tully et al. (2006). In comparison with groups of galaxies, these associations present lower masses and velocity dispersions despite their large size. Their low masses, in addition to their low luminosity, suggest that their mass-to-light ratio is relatively high if these systems are bound systems. Based on this assertion, Tully et al. (2006) infer that these associations are bound but dynamically unevolved systems. They also suggest that they presumably contain DM subhaloes ranging from 10^9 to 10^{10} $M_\odot$, which contain insufficient amounts of gas and stars to be detected at present.

So far, only a few of these associations have been observed and very little is known about their properties. But these systems are of fundamental importance because they could be used as a probe of the cosmological model if a substantial number of them will be detected in future surveys. Currently, the standard paradigm, ΛCDM, is a theory predicting evolution of haloes due to mergers. In fact, at virtually any given moment in cosmic time, DM haloes undergo mergers. The relevant time-scales here are well known. Therefore, it is intriguing to examine the nature of associations that withstand the cosmic forces of tides and gravity.

From the observational point of view, although currently only less than a dozen of these systems of dwarf galaxies are known, their study holds significant importance in anticipation of upcoming galaxy surveys, such as the Dark Energy Spectroscopic Instrument[1] (DESI Collaboration 2016a,b), the Vera C. Rubin Observatory (Ivezić et al. 2019), the 4-metre Multi-Object Spectroscopic Telescope (de Jong et al. 2019), among many others. These surveys hold the promise of providing a highly detailed map of the Local Universe, facilitating the detection of faint galaxies that have remained elusive until now. By detecting these faint galaxies, we anticipate the possibility of identifying new systems exclusively composed of dwarf galaxies. In this sense, our findings will consist of theoretical predictions that await observational confirmation when these future galaxy catalogs become available.

The main goal of this paper is to deepen the theoretical understanding of these associations of dwarf galaxies by analysing the large-scale environment within which they form and evolve and to study how their main dynamical properties vary with the environment. For this, we use the semi-analytic model of galaxy formation semi-analytic galaxies (SAG; Cora et al. 2018) coupled to the $400\,h^{-1}$ Mpc SMALL MULTIDARK PLANCK simulation (SMDPL) based on the Planck cosmology (Klypin et al. 2016). SMDPL simulation is publicly available in the COSMOSIM data base.[2]

This paper is organized as follows. We describe the SMDPLsimulation and the SAG model in Section 2. In Section 3, we define our sample of associations of dwarf galaxies and describe their main properties. Section 4 classifies the large-scale environment and analyses the dependence of the properties of the associations on the environment. In Section 5, we summarize our main results and present our conclusions.

2 HYBRID MODEL OF GALAXY FORMATION

The sample of associations of dwarf galaxies is extracted from a galaxy catalogue constructed by applying a hybrid model of galaxy formation that couples a semi-analytical model of galaxy formation and evolution with a DM-only cosmological simulation. Below, we briefly describe the main aspects of this model.

2.1 Dark matter cosmological simulation

We use the SMDPL DM-only cosmological simulation.[3], which follows the evolution of 3840^3 particles from redshift $z = 120$ to $z = 0$, within a (relatively) small volume (a periodic box of side-length of $400\,\mathrm{Mpc}\,h^{-1}$). This large number of particles within such a volume reaches a mass resolution of $9.63 \times 10^7\,M_\odot\,h^{-1}$ per DM particle (see Klypin et al. 2016 for more details). SMDPL cosmological parameters are given by a flat ΛCDM model consistent with Planck measurements: $\Omega_\mathrm{m} = 0.307$, $\Omega_\mathrm{B} = 0.048$, $\Omega_\Lambda = 0.693$, $\sigma_8 = 0.829$, $n_\mathrm{s} = 0.96$, and $h = 0.678$, (Planck Collaboration 2014).

The ROCKSTAR halo finder (Behroozi, Wechsler & Wu 2013a) is used to identify DM haloes keeping just overdensities with at least $N_\mathrm{min} = 20$ DM particles. There are two classifications of DM haloes: *main host* haloes (detected over the background density) and *subhaloes* (that lie inside other DM haloes). From these haloes, CONSISTENTTREES (Behroozi et al. 2013b) constructs merger tree, by linking haloes and subhaloes forwards and backwards in time to progenitors and descendants, respectively.

[1] https://www.desi.lbl.gov/
[2] https://www.cosmosim.org
[3] doi:10.17876/cosmosim/smdpl/

2.2 Semi-analytic model of galaxy formation SAG

In this project, we follow Yaryura et al. (2020) and use the latest version of the semi-analytic model SAG presented in Cora et al. (2018), based on the model previously presented by Springel et al. (2001). This is an updated and improved version, including the main physical processes required for galaxy formation: gas cooling, star formation in quiescent and bursty modes (being the latter triggered by disc instabilities and mergers), black hole growth, feedback from supernovae and active galactic nuclei (AGN), environmental effects (ram pressure stripping and tidal stripping), chemical enrichment. The circulation of mass and metals among the different baryonic components (hot gas halo, cold gas disc, stellar disc, and bulge) are regulated by ejection and reincorporation mechanisms associated to feedback processes and recycling of stellar mass. We refer the reader to Cora et al. (2018) for a detailed and exhaustive description of the model.

Each SAG galaxy populates a DM halo of the simulation in such a way that central galaxies correspond to main host haloes while satellite galaxies are hosted by subhaloes, according to the information provided by the merger trees. A satellite galaxy is defined as an orphan galaxy when its DM substructure is no longer detected by the halo finder. The position and velocity of orphan galaxies are obtained following the model introduced by Delfino et al. (2022) to calculate the orbital evolution of unresolved subhaloes.[4]

The main galaxy properties provided by SAG are listed in Knebe et al. (2018, see their table A2), although the information of many other properties can be obtained as requested by a given project. The properties used in the current work are: a pointer to the DM halo in which a galaxy orbits; galaxy type (central galaxy, satellite with DM substructure, orphan satellite); positions and velocities of a galaxy; stellar mass of a galaxy, $M_\star$; mass of the main host DM halo in which a galaxy resides, M_{200}. The halo mass is defined as the mass enclosed by a sphere of radius r_{200}, within which the mean density is a factor $\Delta = 200$ times the critical density of the Universe ρ_c, i.e.

$$M_{200}(< r_{200}) = \Delta\rho_c \frac{4\pi}{3} r_{200}^3. \quad (1)$$

To regulate the physical processes involved in the SAGmodel, a set of free parameters is employed: the star formation efficiency (α); the efficiency of SN feedback from stars formed in both the disc and the bulge (ϵ); the efficiency of ejection of gas from the hot phase ($\epsilon_{\rm ejec}$) and of its reincorporation (γ); the growth of super massive black holes and efficiency of AGN feedback ($f_{\rm BH}$ and $\kappa_{\rm AGN}$, respectively); the factor involved in the distance scale of perturbation to trigger disc instability events ($f_{\rm pert}$); and the fraction that determines the destination of the reheated cold gas of a satellite galaxy ($f_{\rm hot,\,sat}$; when the hot gas mass of a satellite drops below a fraction $f_{\rm hot,\,sat}$ of its baryonic mass, the reheated mass and associated metals are transferred to the corresponding central galaxy instead of being transported to the satellite's hot gas halo). The parameter that regulates the redshift dependence of the SNe feedback was not allowed to vary during the calibration process but fixed in 1.3, according to the fit found by Muratov et al. (2015) from the analysis of their cosmological hydrodynamical simulations; this value allows SAG to provide stellar mass and halo mass dependencies of the fractions of local quenched galaxies in better agreement with observational data (Cora et al. 2018, see their fig. 11).

[4]In this work, we use a previous version of the orbital evolution code, where an isothermal sphere models the mass profile of both the host halo and unresolved subhaloes.

Table 1. Best-fitting values of the free parameters of SAG model obtained with the PSO technique. This set of values is obtained from the application of SAG to the merger trees of the sub-box selected from the SMDPL simulation.

Parameter	Best-fitting value
α	0.08
ϵ	0.53
$\epsilon_{\rm ejec}$	0.01
$f_{\rm BH}$	0.07
$\kappa_{\rm AGN}$	1.18×10^{-5}
$f_{\rm pert}$	31.22
γ	0.005
$f_{\rm hot,\,sat}$	0.26

These parameters are calibrated using a set of observed galaxy properties: (i) the stellar mass functions at $z = 0$ and $z = 2$, for which we adopt the compilation data used by Henriques et al. (2015); (ii) the star formation rate distribution function, which is the number density of galaxies in a certain interval of star formation rate; in this case, we use data from a flux-limited sample of galaxies observed with the *Herschel* satellite in the redshift range $z \in [0.0, 0.3]$ (Gruppioni et al. 2015); (iii) the fraction of mass in cold gas as a function of stellar mass; iv) the relation between bulge mass and the mass of the central supermassive black hole (BH). For these two latter relationships, we adopt observational data from Boselli et al. (2014), which is based on a volume-limited sample, within the range $\log(M_\star[M_\odot]) \in [9.15, 10.52]$ in stellar mass, and a combination of the data sets from McConnell & Ma (2013) and Kormendy & Ho (2013), respectively. The best-fitting values of the free parameters of SAG for the SMDPL simulation were selected using the Particle Swarm Optimization (PSO) technique (Ruiz et al. 2015), which are presented in Table 1.

3 ASSOCIATIONS OF DWARF GALAXIES

3.1 Samples

The galaxy samples analysed in this work are obtained from a set of semi-analytical galaxies built by enforcing a minimum stellar and halo mass of $M_\star = 10^{6.8}\,{\rm M}_\odot\,h^{-1}$ and $M_{200} = 10^{9.28}\,{\rm M}_\odot\,h^{-1}$ (equivalent to 20 DM particles), respectively. The final sample has a total of 26 506 948 well resolved, semi-analytical galaxies, with stellar masses ranging between $6.8 < \log_{10}(M_\star[{\rm M}_\odot\,h^{-1}]) < 12.9$ and halo masses ranging between $9.28 < \log_{10}(M_{200}[{\rm M}_\odot\,h^{-1}]) < 15.17$. A well-established percolation algorithm, known as *friends-of-friends* (Huchra & Geller 1982), is used to identify galaxy systems with sizes similar to the observed associations presented in Tully et al. (2006). To define our samples, we follow the procedure described in Yaryura et al. (2020). We use a linking length of $0.4\,{\rm Mpc}\,h^{-1}$ and select systems of galaxies with at least three members. We select this linking length value following Yaryura et al. (2020) who analyse characteristic sizes of systems identified varying the linking length parameter between $0.3\,{\rm Mpc}\,h^{-1}$ and $0.5\,{\rm Mpc}\,h^{-1}$. Characteristic sizes of the systems are sensitive to the chosen linking length, being more extended when they use a greater linking length value. Comparing with the observational results presented by Tully et al (2006), they conclude that $0.4\,{\rm Mpc}\,h^{-1}$ is the best choice for the analysis of these associations. In a first instance, we do not include the velocity of the systems as a selection criteria since our main objective is to mimic observation. We want to identify systems with properties comparable to the observations but considering the fewest possible restrictions in their selection.

Table 2. Different samples analysed throughout this paper, described in detail in Section 3.1. First column shows the name of the sample. Second column indicates the maximum stellar mass threshold. Third column indicates if galaxy members belong to the same main host halo, to different ones or to a mix of both previous situations. Fourth column shows the number of systems in each sample. Fifth, sixth, and seventh columns indicate the number of systems with 3, 4, and 5 or more members, respectively.

	$M_\star$max ($M_\odot/h$)	Main DM halo	$N_{\rm systems}$	N = 3	N = 4	$N \geq 5$
Dwarf_associations	$10^{9.0}$	Different	308 250	211 243	61 849	35 157
Dwarf_mix	$10^{9.0}$	Mix	257 277	125 006	66 487	65 783
Dwarf_groups	$10^{9.0}$	Same	40 789	35 243	4622	923
All_associations	∞	Different	429 444	275 708	90 465	63 270
All_mix	∞	Mix	890 712	220 785	163 809	506 117
All_groups	∞	Same	153 368	99 957	30 247	23 163

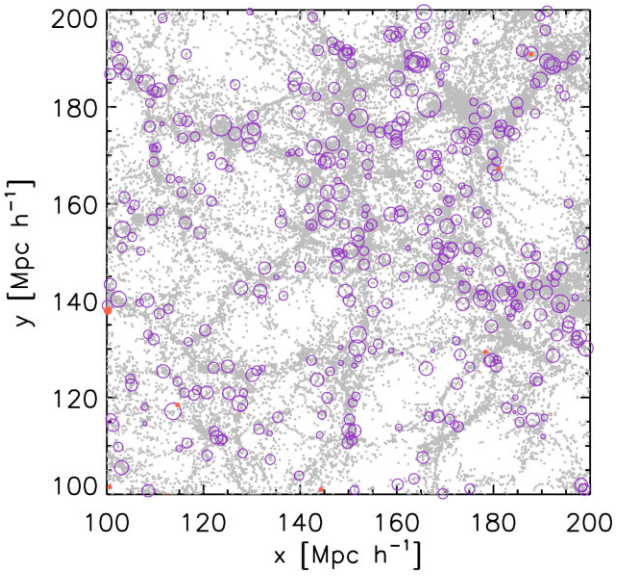

Figure 1. Spatial projected distribution of our semi-analytical galaxies (grey small dots) in a slice of 10 Mpc h^{-1} thickness. Purple empty circles show the position of the centre of mass of systems identified for the sample *Dwarf_associations*, while orange filled circles correspond to systems identified for the sample *Dwarf_groups*. Systems in *Dwarf_associations* dominate in number and there are very few systems in *Dwarf_groups*, so it is difficult to see them. For both samples, circle radius indicates $5R_I$, where R_I is the inertial radius defined in equation (2). We do not show systems of *Dwarf_mix* sample to make the plot clearer.

As we are interested in systems made up only of dwarf galaxies, we remove those systems that have one (or more) galaxy member more massive than a stellar mass threshold $M_{\star,\rm max}$. In this paper, we consider dwarf galaxies as those galaxies less massive than $M_{\star,\rm max} = 10^{9.0}$ $\rm M_\odot\, h^{-1}$ (we check that our results do not vary significantly if we consider a more restrictive value as $M_{\star,\rm max} = 10^{8.5}$ $\rm M_\odot\, h^{-1}$, or a less restrictive value as $M_{\star,\rm max} = 10^{9.5}$ $\rm M_\odot\, h^{-1}$). Once we selected systems made up only of dwarf galaxies, and following the classification made by Yaryura et al. (2020), we split the sample into three different sub-samples according to the following conditions: (i) systems with all their galaxy members belonging to the same main DM halo; (ii) systems with all their galaxy members belonging to different main host DM haloes; (iii) systems for which some of the galaxies belong to the same main DM halo, but others belong to different main host haloes. We refer to these respective sub-samples as: (i) *Dwarf_groups*, (ii) *Dwarf_associations*, and (iii) *Dwarf_mix*. It is important to note that each system belongs to only one of these sub-samples. For comparison, we also consider samples without restriction in the maximum value of the stellar mass of member galaxies. In those cases, the samples are called *All_groups*, *All_associations*, and *All_mix*, according to the previously described criterion of belonging to a DM halo. Table 2 summarizes these samples.

Fig. 1 shows the spatial projected distribution of semi-analytical galaxies (small grey dots) in a slice of 10 Mpc h^{-1} thickness. Open purple circles show the position of the systems in the sample *Dwarf_associations*, while orange filled circles correspond to systems identified in the sample *Dwarf_groups*. To make the plot clearer, the circle radius indicates $5R_{\rm I}$, where $R_{\rm I}$ is the inertial radius considered as an indicator of the size of the system, defined by

$$R_{\rm I} = \left(\sum_i^N r_i^2 / N \right)^{1/2} , \qquad (2)$$

where r_i is the three–dimensional distance of a galaxy from the system centroid and the sum for each system is performed over all members (N). From this plot, it is evident that associations of dwarf galaxies, with all their galaxy members belonging to different main host DM haloes, are much more numerous and noticeably larger than systems, with all their galaxy members belonging to the same main host DM halo. It is expected that *Dwarf_associations* are more numerous than *Dwarf_groups* due to the resolution limit. Requiring a minimum halo mass of $M_{200} = 10^{9.28}\,\rm M_\odot\, h^{-1}$, there are large number of dwarf galaxies that are not resolved and therefore are not taken into account. These ignored dwarf galaxies, which accompany the central galaxy of the main host halo, could form groups of dwarf galaxies that are dismissed in our analysis. However, although resolution effects can affect differently groups and associations, their relative abundance is not the main subject of our paper which focalizes in their dynamical and environmental properties.

To identify which of the previously defined samples most accurately reproduce the observed data, we analyse different dynamical properties and attempt to match the observed size-stellar mass relation from Tully et al. (2006). The left-hand panel of Fig. 2 shows the size of the systems [$R_{\rm I}$, defined in equation (2)] as a function of the stellar mass of the system ($M_\star^{\rm sys}$), defined as the sum of the galaxy stellar mass of all the galaxies defining each association or group. For comparison, we also plot the size of the observed dwarf galaxy associations taken from Tully et al. (2006; black filled circles). This comparison is based on the B-band luminosity, L_B, of these observed systems, assuming a mass–luminosity ratio equal to 1. Notice that assuming a different value for the mass–luminosity ratio would only cause a horizontal shift in our results, which does not modify the conclusions. Systems in the sample *Dwarf_associations* do much better in reproducing the empirical characteristic sizes of the observational sample of dwarf galaxies associations, in agreement with the results presented by Yaryura et al. (2020). From this figure, it

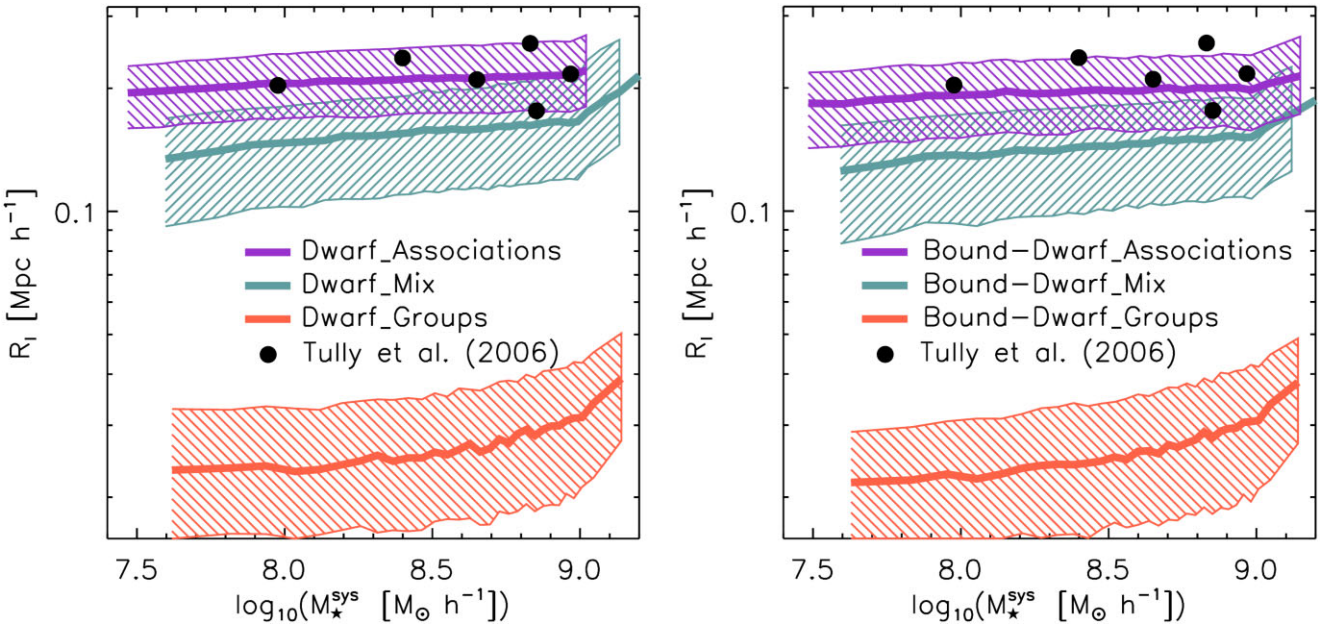

Figure 2. Left-hand panel: Size of dwarf galaxy systems (R_I) as a function of the stellar mass of the system ($M_\star^{\rm sys}$). Different coloured lines correspond to different samples: *Dwarf_associations* (purple line), *Dwarf_mix* (green line), and *Dwarf_groups* (orange line). Solid lines show median values, taking equal number of bins in $M_\star^{\rm sys}$. Shaded regions cover from 25 per cent to 75 per cent for each sample. They are compared with observational results for dwarf galaxy associations taken from Tully et al. (2006, black filled circles), assuming for them a factor equal to one in the mass-to-light ratio. Right-hand panel: Idem as left-hand panel but considering sub-samples of only gravitationally bound systems: *Bound–Dwarf_associations* (purple line), *Bound–Dwarf_mix* (green line), and *Bound–Dwarf_groups* (orange line).

is evident that systems in the sample *Dwarf_groups* are systematically smaller than systems in the sample *Dwarf_associations* by a factor of ∼5.

Associations presented by Tully et al. (2006) are systems identified from the spatial distribution of dwarf galaxies, so we do not have information regarding the full dynamics of these systems. As a next step and taking advantage of the information provided by simulations, we estimate the binding energy of our theoretical systems compound only by dwarf galaxies to deduce whether they are gravitationally bound. Then, we analyse subsamples of previously described samples (*Dwarf_associations*, *Dwarf_mix*, and *Dwarf_groups*) considering only gravitationally bound systems. We estimate the binding energy of the systems by considering the contribution of each member galaxy, classifying a system as gravitationally bound if its binding energy is negative. For consistency, we name these sub-samples as *Bound–Dwarf_associations* (96 902 systems, ∼31 per cent of the original sample *Dwarf_associations*), *Bound–Dwarf_mix* (181 046 systems, ∼70 per cent of the original sample), and *Bound–Dwarf_groups* (39 048 systems, ∼96 per cent of the original sample). The right-hand panel of Fig. 2 shows same as left-hand panel but considering sub-samples of only gravitationally bound systems. There are no significant differences between both panels, indicating that the sample of *Bound–Dwarf_associations* show more similar results to the observational sample of dwarf galaxies associations, same as left-hand panel.

It is evident that observed associations have characteristic sizes comparable with *Dwarf_associations*, from where we could infer that member galaxies of the observed associations would be located in different main DM haloes. Furthermore, if the observed associations were in the same DM halo, it would likely be a large halo (due to the extended size of these systems), making it unlikely that the central galaxy is a dwarf galaxy. Therefore, based on Fig. 2, henceforth, we concentrate on the samples *Dwarf_associations* and its sub-sample *Bound–Dwarf_associations* to analyse how the environment affects their main dynamical properties. The rest of the samples are used for comparison.

To better understand whether galaxy members of *Dwarf_associations* are preferably central galaxies, satellite galaxies with DM substructure, or orphan galaxies, we study the internal structure of these associations. We find that 90 per cent of these systems are composed of three or four members, most of which are central galaxies (∼97.5 per cent) while the rest are orphan galaxies (∼2.5 per cent). Fig. 3 shows the number of galaxy systems as a function of the number of members per system. Different coloured lines correspond to different samples: *Dwarf_associations* (purple line), *Dwarf_mix* (green line), and *Dwarf_groups* (orange line). From this figure, it is evident that most of the systems are composed just of three or four members: 90 per cent for *Dwarf_associations*, 75 per cent for *Dwarf_mix*, and 98 per cent for *Dwarf_groups*.

4 ENVIRONMENTAL EFFECTS

4.1 Classification of the environment

In the last few years, many papers have found evidence of properties of galaxies and systems of galaxies that depend on the environment in which they reside (Dressler 1980; Kauffmann et al. 2004; Blanton et al. 2005; O'Mill et al. 2008; Peng et al. 2010; Wetzel et al. 2012; Zheng et al. 2017; Wang et al. 2018; Duplancic et al. 2020, among others). There are many different methods to classify large-scale cosmic matter distribution (see Libeskind et al. 2018, for a review). Most of these define the Hessian matrix from the density, velocity, or potential field using a fixed finite grid. Then, this matrix is

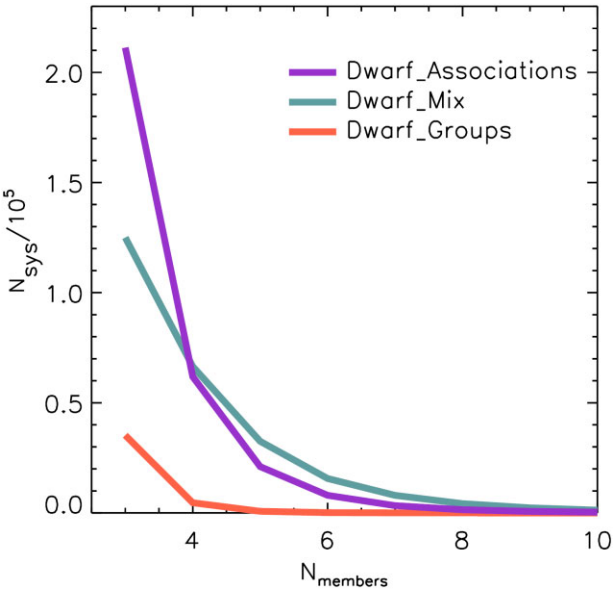

Figure 3. Number of galaxy systems as a function of the number of members per system. Different coloured lines correspond to different samples: *Dwarf_associations* (purple line), *Dwarf_mix* (green line), and *Dwarf_groups* (orange line).

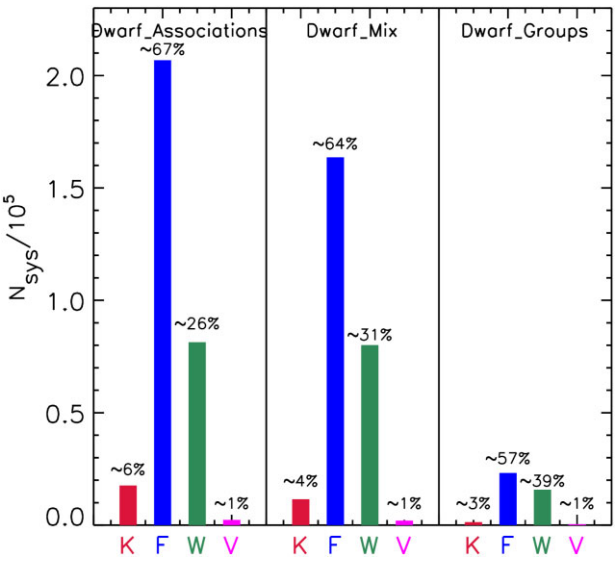

Figure 4. Number of systems located in each large-scale environment classification: knot (red bars), filament (blue bars), wall (green bars), and void (magenta bars); for the samples *Dwarf_associations* (left-hand panel), *Dwarf_mix* (middle panel), and *Dwarf_groups* (right-hand panel). Percentage values with respect to the total of each sample are indicated above each bar.

diagonalized to determine their eigenvectors and eigenvalues, which give information about the principal directions and strength of local collapse or expansion. The main disadvantage of these methods is the finite resolution assigned by a finite grid. Wang et al. (2020) presented an improvement to these methods given by an adaptive interpolation guaranteeing higher resolution. We apply this method to our samples and refer the reader to Wang et al. (2020) for a detailed description of their method.

To characterize the environment where associations of dwarf galaxies are found, we use the eigenvalues estimated from both the tidal tensor (e.g. Hahn et al. 2007a) and shear velocity (Hoffman et al. 2012) of the DM particle distribution of the parent simulation SMDPL. We define four types of environment, knot, filament, wall, or void, based on the number of eigenvalues larger than a chosen threshold (λ_{th}). If we adopt the nomenclature $\lambda_1 < \lambda_2 < \lambda_3$ for the smallest, intermediate, and largest, respectively, then we define

(i) Knot: if $\lambda_{th} < \lambda_1$
(ii) Filament: if $\lambda_1 < \lambda_{th} < \lambda_2$
(iii) Wall: if $\lambda_2 < \lambda_{th} < \lambda_3$
(iv) Void: if $\lambda_3 < \lambda_{th}$

We use a grid of 400^3 cells and three different specific smoothing lengths $l = 1,\ 2$ or 4 Mpc h^{-1} over the tidal and shear velocity tensor. Then, we estimate the three eigenvalues for each cell. According to the position of the centre of mass of each association, we assign to it the eigenvalues of the cell where it is located. Following Wang et al. (2020), we adopted a threshold $\lambda_{th} = 0$ to define the four classifications. In this way, each association belongs to a single environment: void, wall, filament, or knot.

The distribution of associations among the different environments depends on the choice of the smoothing length, as shown in Appendix A. We have checked that the results obtained in this work do not depend either on the field used to classify the environment (tidal tensor or shear velocity), or on the smoothing length ($l = 1,\ 2$ or 4 Mpc h^{-1}). Therefore, for simplicity and clarity, the results of this paper will be presented only for the tidal tensor and for the smoothing length $l = 1$ Mpc h^{-1}. This smoothing length represents about five times the median size of the associations, so it is a sufficient volume to analyse their environment.

Note that taking $\lambda_{th} = 0$, this classification takes into account only the sign of the eigenvalues and not the ratio between the eigenvalues. Furthermore, the tidal tensor eigenvalues refer to the directions of differential motion, namely compression and expansion. This should not be confused with the ellipsoidal shape of the mass distribution, defined by the inertia tensor. In general, however, there is a correlation and an alignment between the inertia tensor and the tidal tensor eigenvalues (Porciani, Dekel & Hoffman 2002). A knot means that the three eigenvalues are pointing inwards, i.e. the system is collapsing; a filament means that two eigenvalues are collapsing and one expanding (the expansion direction corresponds to the filament's 'spine'). A wall means that two eigenvalues are expanding and one is collapsing (which corresponds to the sheet normal), and a void means that the three eigenvalues are pointing outwards, i.e. the system is expanding.

According to this large-scale environment classification (knot, filament, wall, and void), most of the associations in the *Dwarf_associations* sample are located in filaments (~67 per cent), followed by the wall environment (~26 per cent), while a minority fraction is in knots (~6 per cent) and voids (~1 per cent). We specify percentage values for systems with all their galaxy members belonging to different main host DM haloes, i.e. the *Dwarf_associations* sample, because they are the focus of our work, but these values do not change significantly for other samples. Fig. 4 shows the number of systems located in each large-scale environment classification, for the samples *Dwarf_associations*, *Dwarf_mix* and *Dwarf_groups* (percentage values are indicated above each bar). For the rest of the samples, these values do not change significantly either. For example, for the *All_associations* sample, ~69 per cent of the systems are located in filaments, ~24.5 per cent in walls, ~6 per cent in knots, and only ~0.5 per cent in voids. Likewise, if we consider systems without a restriction in the maximum value of the stellar mass of their member galaxies and without distinction of the halo in which

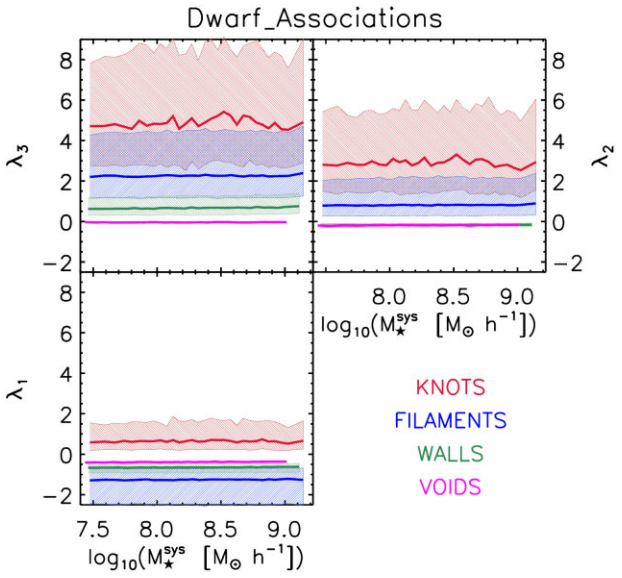

Figure 5. Values of the three eigenvalues as a function of the stellar mass of associations for the sample *Dwarf_associations* split according to the environment in which they reside as indicated by the legends. Coloured solid lines show median values of eigenvalues taking equal number of bins in $M_\star^{\rm sys}$. Shaded regions cover from 25 per cent to 75 per cent for each sample.

their member galaxies are hosted (i.e. *All_associations* + *All_mix* + *All_groups*), the percentages are very similar: ∼70 per cent in filaments, ∼22 per cent in walls, ∼7.5 per cent in knots, and ∼0.5 per cent in voids. Although it is not a strictly direct comparison, we can compare these percentages with the mass fraction assigned to a given environmental classification. As we have already mentioned above, a variety of methods have been developed to classify the cosmic web (see Libeskind et al. 2018, for a review). As these methods identify the web components differently, it is not surprising that there are significant discrepancies in these fractions. Despite these differences, for most of these methods, the largest mass fraction is found in filaments (ranging from ∼30 per cent to ∼90 per cent depending on the method), followed by walls or nodes depending on the method, while the lowest mass fraction is found in voids (less than 10 per cent in most of these methods). Despite not being a direct comparison and taking into account the differences in the percentages, our results follow the same trend presented by these works.

Fig. 5 shows values of the three eigenvalues as a function of the total stellar mass of the systems ($M_\star^{\rm sys}$), for the sample *Dwarf_associations*, split according to the environment in which they reside as indicated by the legends. Coloured lines show median values of eigenvalues taking equal number of bins in $M_\star^{\rm sys}$, while shaded regions cover from 25 per cent to 75 per cent for each sample. The eigenvalues do not show a significant dependence on the stellar mass of the association. From this figure, the sign of each eigenvalue is evident, indicating the direction of the tidal field (collapse if positive and expansion if negative) taking into account the adopted threshold $\lambda_{\rm th} = 0$ for the classification of the structure in the cosmic web.

4.2 Properties of dwarf galaxy associations

To analyse the environmental effects on the associations of dwarf galaxies, we study how their main dynamical properties vary according to the environment in which these particular systems reside. As the main intrinsic properties of our systems, we compute the inertial radius [$R_{\rm I}$, defined in equation (2)] as an indicator of the size of the system, the velocity dispersion (σ), and the stellar mass of the system ($M_\star^{\rm sys}$). The velocity dispersion is computed through the unbiased sample variance of the sample for all member galaxies, defined by

$$\sigma = \left[\sum_i^N v_i^2/(N-1)\right]^{1/2}. \quad (3)$$

where v_i is the one-dimensional velocity difference between a galaxy and the mean velocity of the system.

Fig. 6 shows the main dynamical properties of our systems ($R_{\rm I}$ and σ) as a function of the total stellar mass of the association ($M_\star^{\rm sys}$) for systems in the sample of dwarf galaxy associations (*Dwarf_associations*, left-hand panels). Coloured lines show median values of each property taking an equal number of bins in $M_\star^{\rm sys}$. Each colour corresponds to a different environment (knots, filament, walls, and voids), as indicated by the legends. Top-right panels show the ratio between the DM particles density ρ in the grid cell where the system is located and the mean density ($\rho/\overline{\rho}$) as a function of the stellar mass of the system. This ratio is related with eigenvalues by $\rho/\overline{\rho} - 1 = \lambda_1 + \lambda_2 + \lambda_3$. As expected, it is clear that knots correspond to the highest densities, followed by filaments, then walls and finally voids, which correspond to the lowest density. From the results for the associations (*Dwarf_associations* sample), it is evident that the velocity dispersion depends strongly on the environment where the association is located. Associations have a very low velocity dispersion ($\sigma \sim 20\,{\rm km\,s^{-1}}$) if found in voids, which increases up to $\sigma \sim 140\,{\rm km\,s^{-1}}$ as we move to knots, going through walls and filaments. As associations are composed exclusively of galaxies that do not live in the same DM halo, they are somehow tracing the velocity dispersion of the environment where they are located: knot, filament, wall, or void. This dependence of velocity dispersion on the environment has already been previously studied in some published works. Among the most recent, we can mention Taverna et al. (2023), who study the effects of different global environments on the properties of Hickson-like compact groups of galaxies (CGs) identified in the Sloan Digital Sky Survey Data Release 16 (Ahumada et al. 2020). They found that CG velocity dispersion increases with the density of the environment they inhabit, since the median velocity dispersion observed for CGs in the highest-density environments almost doubles that of observed for CGs in the lowest-density environments. Furthermore, we can mention the results presented by Ruiz, Alfaro & Garcia Lambas (2019) who compare pairwise velocity (w) distributions for all galaxies with pairwise velocity distributions for galaxies located in void regions. They found $w \sim 500\,{\rm km\,s^{-1}}$ for all galaxies, while for void galaxies the pairwise velocity dispersions are in the range $w \sim 50 - 70\,{\rm km\,s^{-1}}$, roughly one order-of-magnitude smaller. They found these differences in both the observations and in the simulated galaxies. Our results are in accordance with these results in the sense that the velocity dispersion shows the same trend, being significantly smaller in low-density regions than in high-density regions. Moreover, this progressive increase of the values of the velocity dispersion through different environments, regardless of the total stellar mass of the association, is also accompanied by an increasing trend of the velocity dispersion with increasing $M_\star^{\rm sys}$, and this trend is more pronounced for associations residing in filaments and almost non-existent in associations located in knots. In relation to the size of the associations, there are no systematic effects of the environment on the size of associations.

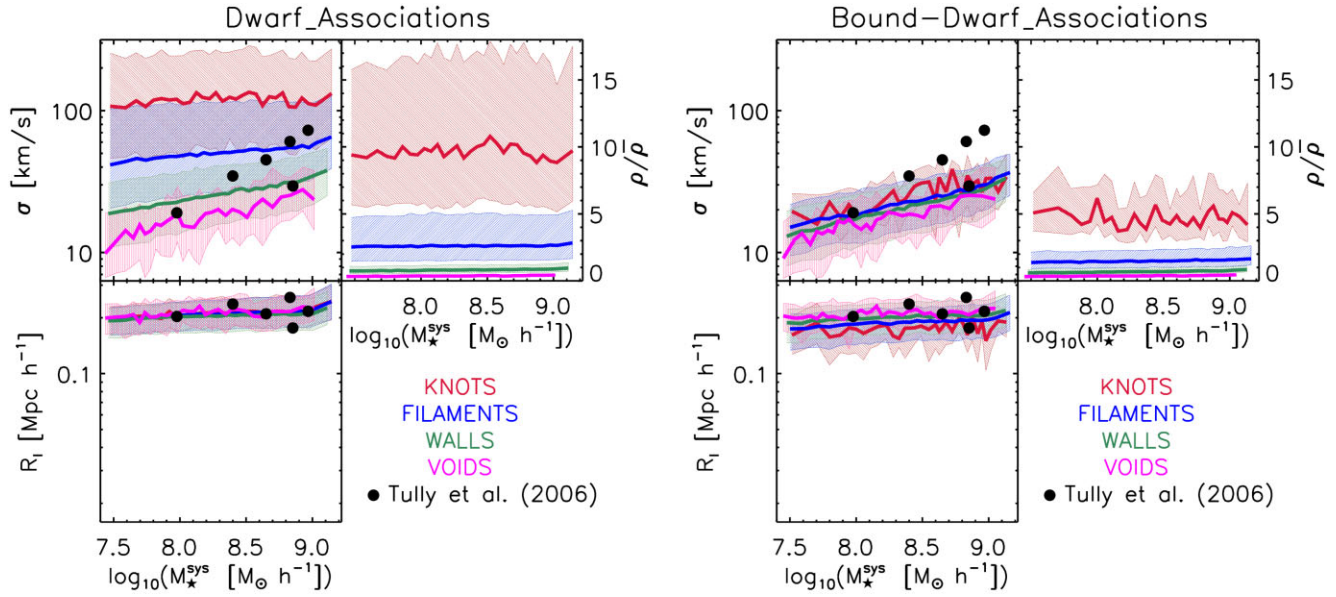

Figure 6. Left-hand panels: Dynamical properties of associations as a function of the stellar mass of the association ($M_\star^{\rm sys}$) for systems in the sample *Dwarf_associations*: velocity dispersion (σ, top left), size ($R_{\rm I}$, bottom left) and the ratio between the DM particles density ρ in the grid cell where the system is located and the mean density ($\rho/\bar{\rho}$, top right). Solid lines show median values of each property, taking equal number of bins in $M_\star^{\rm sys}$. Each colour corresponds to a different environment (knots, filaments, walls and voids) as indicated in the legends. Shaded regions cover from 25 per cent to 75 per cent for each sample. Results for simulated associations of dwarf galaxies are compared with observational results taken from Tully et al. (2006, black filled circles), assuming for the latter a factor equal to one in the mass-to-light ratio. Right-hand panels: Idem as left-hand panels but considering a sub-sample with only gravitationally bound systems (*Bound–Dwarf_associations*).

Table 3. Probability of each observed association to belong to one environment. First column indicates the association. Second column shows the velocity dispersion of the association. Third, fourth, fifth, and sixth columns indicate the probability of each observed association to belong to one web type environment: knot, filament, wall, and void, respectively. The highest probability for each association is highlighted in bold type.

Observed Associations	σ (km s^{-1})	Knot	Filament	Wall	Void
1	19.05	6 per cent	16 per cent	34 per cent	**44 per cent**
2	29.44	6 per cent	21 per cent	33 per cent	**40 per cent**
3	34.64	10 per cent	26 per cent	**36 per cent**	28 per cent
4	45.03	17 per cent	30 per cent	**32 per cent**	20 per cent
5	60.62	24 per cent	**35 per cent**	29 per cent	12 per cent
6	72.75	34 per cent	**39 per cent**	27 per cent	0 per cent

Compared with observational results, the dynamical properties of most of the observed dwarf galaxy associations presented by Tully et al. (2006; black filled circles) are compatible at first glance with a filament-like (three systems) or wall-like (two systems) environment, while just one association is compatible with a void-like environment. In a deeper analysis, we compute the probability of each association to belong to a web-type environment classification. We estimate the probability distribution function (PDF) of velocity dispersion for each web-type environment classification, regarding bins of mass. Taking this distribution into account, we assign a probability value for each observed association. This probability is shown in Table 3, where the highest probability for each association is highlighted in bold type. The associations are stored in increasing order of their velocity dispersion. Considering the highest values of these probabilities, it appears that two associations belong to the void-like environment (Association 1 and Association 2), two belong to the wall-like environment (Association 3 and Association 4), and two belong to the filament-like environment (Association 5 and Association 6). Nevertheless, these highest probabilities are not significantly larger compared to the others, thereby indicating that the membership in a given web-type classification is not particularly evident. This is primarily due to the large scatter in velocity dispersion for each environment, as evidenced by the shaded regions in the figure. Another important thing to note is that, as the velocity dispersion of the associations increases, the probability of belonging to denser environments also increases.

We also analyse systems in the sample built without restriction in the maximum value of the galaxy stellar mass (*All_associations*), and there are not significant differences between their results and those previously described. Due to the similarities between results, we do not show the latter ones to make the discussion clearer. In brief, these results show that the increase of σ with the density of the environment does not happen only in associations of dwarf galaxies but is noticed in all systems where their member galaxies belong to different DM haloes.

Going even further, right-hand panels of Fig. 6 show the same as left-hand panels considering only gravitationally bound systems (*Bound–Dwarf_associations*). For this sample, it is evident that the dependence of velocity dispersion on the environment where the association is located is noticeably attenuated. The velocity dispersion covers a narrow range around low velocity dispersions, between $\sigma \sim 10\,{\rm km\,s^{-1}}$ and $\sigma \sim 30\,{\rm km\,s^{-1}}$, depending on the mass of the system, with minimal differences according to the environment in which they are located. Although a trend is slightly visible, it is too weak. Therefore, we can infer that the velocity dispersion of gravitationally bound systems does not depend on the environment in which they reside. Comparing with observational results, the velocity dispersion of at least half of the observed dwarf galaxy associations

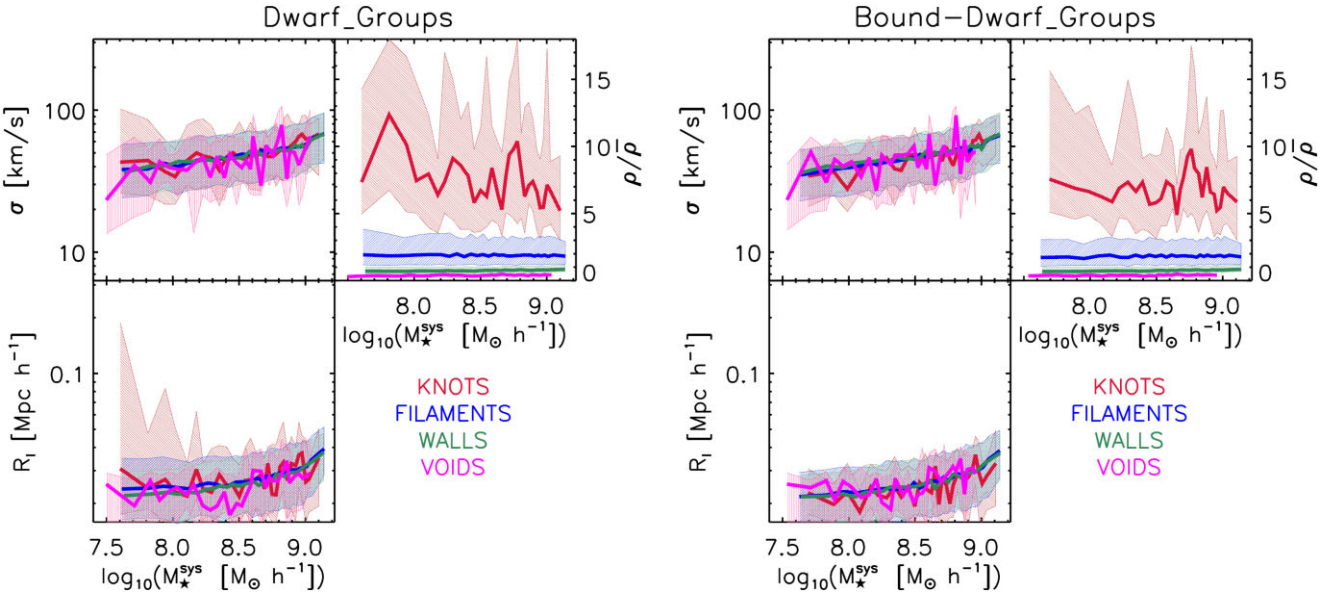

Figure 7. Left-hand panels: Dynamical properties of groups of galaxies as a function of the stellar mass of the group ($M_\star^{\rm sys}$) for systems in the sample *Dwarf_groups*: velocity dispersion (σ, top left), size ($R_{\rm I}$, bottom left), and the ratio between the DM particles density ρ in the grid cell where the system is located and the mean density ($\rho/\bar{\rho}$, top right). Solid lines show median values of each property, taking an equal number of bins in $M_\star^{\rm sys}$. Each colour corresponds to a different environment (knots, filaments, walls, and voids) as indicated in the legends. Shaded regions cover from 25 per cent to 75 per cent for each sample. Right-hand panels: Idem as left-hand panels but considering a sub-sample with only gravitationally bound systems: *Bound–Dwarf_groups*.

presented by Tully et al. (2006; black filled circles) are not compatible with our results. This would indicate that these observed associations could be non-gravitationally bound systems.

Fig. 7 shows the same relationships as Fig. 6 considering different samples. Panels in the left box correspond to systems of sample *Dwarf_groups*, while panels in the right box correspond to systems of sample *Bound–Dwarf_groups*, a sub-sample of the former containing only gravitationally bound systems. In these cases, unlike the samples shown in the previous figure, all member galaxies belong to the same main host DM halo. It is noticeable that the typical size of these systems is much smaller than those of samples *Dwarf_associations* and *Bound–Dwarf_associations* shown in Fig. 6. Moreover, the dependence of σ on the environment in which the systems reside disappears. It is evident that the behaviour of σ with respect to the stellar mass of the system is very similar for all environments. As expected, the results of these two samples are very similar between them, due to the fact that *Bound–Dwarf_associations* is a sub-sample of *Dwarf_groups*, which contains about ∼96 per cent of their groups. The remaining ∼4 per cent, that is, the unbound groups of dwarf galaxies, mainly consist of subgroups found within larger DM haloes. We also analyse systems in the sample built without an upper limit in their stellar mass (*All_groups*), and there are no significant differences between their results and those just described. Again, we avoid showing the results of this sample for a less confusing discussion. So, in summary, velocity dispersion does not depend on the environment when all galaxy members of the system belong to the same main DM halo.

Comparing results from Figs 6 and 7, we infer that, when estimating the velocity dispersion σ for systems that belong to the *Dwarf_associations* sample, we are actually estimating the velocity dispersion of the environment in which the associations are immersed, immediately surrounding them, and not of the system itself. Since galaxy members of these systems belong to different main DM haloes, they are located far from each other. When estimating velocity dispersions of a set of galaxies that are far away from each other, the properties of the environment inevitably affect this estimation. This occurs not only for associations of dwarf galaxies but also for all systems where all their member galaxies belong to different main DM haloes (*Dwarf_associations* and *All_associations* samples). In contrast, when we consider gravitationally bound systems, the difference in the velocity dispersion with the environment is noticeably attenuated, completely disappearing if we consider systems where all their member galaxies belong to the same main DM halo. This is true for systems built up only of dwarf galaxies and for systems without restriction in the stellar mass of their member galaxies, i.e. *Bound–Dwarf_associations*, *Bound–Dwarf_groups*, *Dwarf_groups*, and *All_groups* samples. In summary, considering systems whose galaxies belong to the same main DM halo or gravitationally bound systems (despite the fact that their member galaxies may belong to different main DM haloes), the environment does not play a fundamental role when we estimate the velocity dispersion of their member galaxies. The size of dwarf galaxy systems are directly related to the DM halo in which galaxies reside, while the velocity dispersion of dwarf galaxy systems are directly related to the binding energy of the system and not to the environment in which the DM halo is found within the cosmic web.

The results that we have just reached can be better visualized by Fig. 8. Here, the velocity dispersion (σ) of the galaxy system as a function of the density field of the environment normalized by the mean density ($\rho/\bar{\rho}$) is shown for different samples. Left-hand panel shows *Dwarf_associations* (shaded regions) and *Dwarf_groups* (solid lines) samples, residing in different environments (indicated by the colour code). Shaded regions cover from 25 per cent to 75 per cent of each sample of associations of dwarf galaxies; for dwarf groups, we show only median values (i.e. corresponding to 50 per cent of the sample) to make the figure clearer. In the case of *Dwarf_associations*, the dependence of the velocity dispersion on density is remarkable.

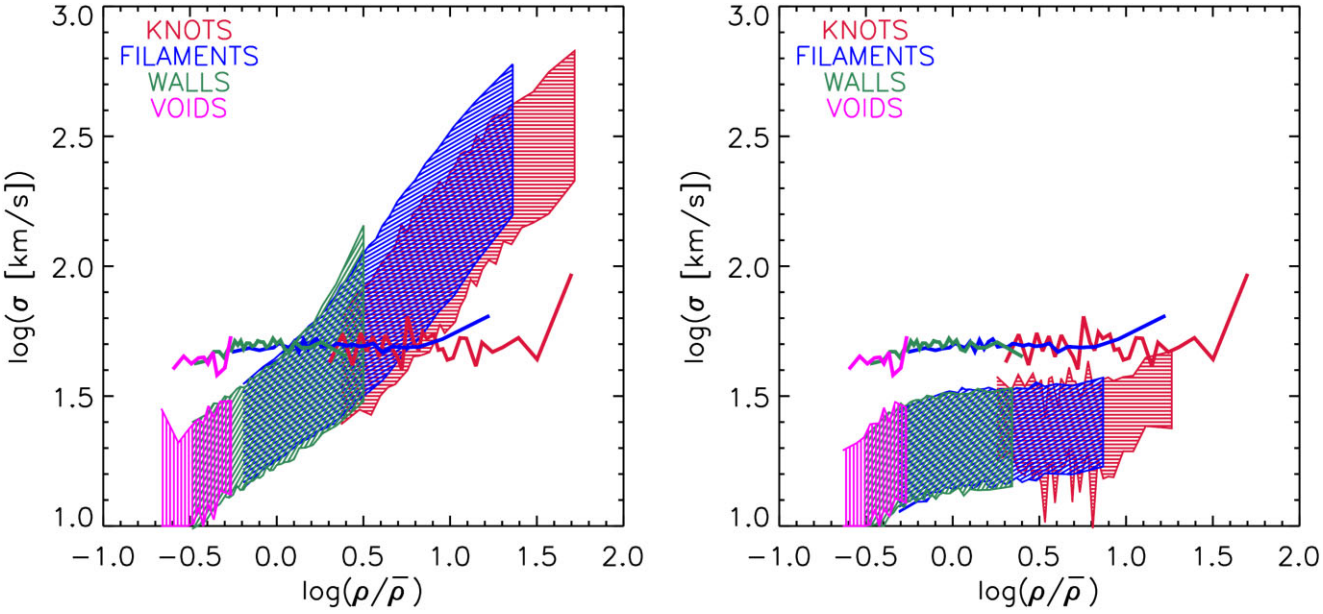

Figure 8. Left-and panel: Velocity dispersion (σ) as a function of DM particle density ρ in the grid cell where the system is located divided by the mean density ($\rho/\bar{\rho}$), shown for two different samples, *Dwarf_associations* (shaded regions) and *Dwarf_groups* (solid lines), for four different environments, as indicated by the colour code. Shaded regions cover from 25 per cent to 75 per cent for the *Dwarf_associations* sample. For the case of *Dwarf_groups*, we show only the median values (i.e. corresponding to 50 per cent of the sample) to make the plot clearer. Right-hand panel: Idem as left-hand panel but considering sub-samples with only gravitationally bound systems: *Bound–Dwarf_associations* and *Bound–Dwarf_groups*.

As the density of the system environment increases, the velocity dispersion of the system also increases. On the other hand, it is clear that the velocity dispersion of *Dwarf_groups* does not depend on the density of the environment in which the system resides. As the density of the system environment increases, the velocity dispersion does not show significant changes. This shows that the velocity dispersion of a system where all its member galaxies belong to different main DM haloes depends strongly on the environment in which the system is located. In contrast, the velocity dispersion of a system where all its member galaxies belong to the same main DM halo does not depend on the environment of the system. On the other side, right-hand panels show samples where all systems are gravitationally bounded: *Bound–Dwarf_associations* (shaded regions) and *Bound–Dwarf_groups* (solid lines) samples. This comparison shows that velocity dispersion does not significantly depend on the environment when we restrict our samples to gravitationally bound systems. This figure confirms that the velocity dispersion of dwarf galaxy systems are directly related to the binding energy of the system and not to the environment in which the DM halo is found within the cosmic web, regardless whether member galaxies are hosted by the same main DM halo or by different main DM haloes.

5 CONCLUSIONS

We analyse how the dynamical properties of associations of dwarf galaxies depend on their environment. Within the ΛCDM cosmological context, we identify these particular systems in the high-resolution DM-only SMDPL simulation (Klypin et al. 2016), coupled to the SAG semi-analytical model of galaxy formation (Cora et al. 2018). We compare associations of dwarf galaxies, where all their members belong to different main DM haloes, with close groups of dwarf galaxies hosted by a single massive DM halo. From Yaryura et al. (2020), we know that the so-called defined associations of dwarf galaxies are the systems that best reproduce the dynamical properties of observed associations presented by Tully et al. (2006). That is why studying associations of dwarf galaxies is our main objective.

We classify the environment into the four different categories of knots, filaments, walls, and voids and analyse its effect on the main properties of the associations and groups of dwarf galaxies. Most dwarf galaxies associations are located in filaments (∼67 per cent), followed by walls (∼26 per cent), knots (∼6 per cent), and voids (∼1 per cent). So far, only seven associations of dwarf galaxies have been observed (Tully et al. 2006). Based on the observed velocity dispersion, we conclude that three of them are most compatible with a filament-like environment, two with a wall-like environment, while just one is most compatible with a void-like environment. Based on the PDF of the velocity dispersion of associations in different environments, we estimated the probabilities of the observed associations to be located in a specific environment (Table 3) and found that they tend to be located in low-density environment (voids, walls up to filaments) and most probably cannot be found in knots. It is worth noting that as the velocity dispersion of the associations increases, so does the probability of belonging to denser environments.

When we analyse the dependence of the dynamical properties of the associations of dwarf galaxies on the environment, we find that the velocity dispersion strongly depends on the environment. Associations have a very high-velocity dispersion ($\sigma \sim 140$ km s^{-1}) if located in knots, which decreases to $\sigma \sim 20$ km s^{-1} as we reach voids, going through filaments and walls. This dependency occurs in systems composed exclusively of dwarf galaxies as well as in systems with no restriction on the maximum value of the stellar mass of their member galaxies. Since the members of the associations belong to different DM haloes, these galaxy systems could be considered as large-scale mass distribution tracers. The velocity dispersion of these galaxies reflects the velocity dispersion of the environment (knot, filament, wall, or void) in which they reside. Therefore, large-scale

environment plays a fundamental role in determining the dynamical properties of associations.

Being more restrictive in the definition of associations, requiring them to be gravitationally bound systems, our results change significantly. When we consider a sub-sample of associations of dwarf galaxies, with only gravitationally bound systems (∼30 per cent of the total sample of associations of dwarf galaxies), the dependence of the velocity dispersion on the environment is strongly attenuated. This indicates that the environment significantly influences the dynamical properties of systems only when they are not physically bound systems. Comparing with observational results presented by Tully et al. (2006), the velocity dispersion of most of these associations is not compatible with that of the bound systems, which could indicate that these observed associations would not be gravitationally bound systems.

When we focus on the groups of dwarf galaxies, defined as systems where all member galaxies belong to the same main DM halo, we do not find any dependence of the velocity dispersion on the environment. About ∼96 per cent of the groups are gravitational bound systems. So, the dynamical properties of these groups are not influenced by the environment where they reside.

ACKNOWLEDGEMENTS

We would like to thank the referee for carefully reading the manuscript and making a lot of suggestions that improved our paper substantially. The SMDPL simulation was performed at LRZ Munich within the pr87yi project. The authors gratefully acknowledge funding for this project from the Gauss Centre for Supercomputing e.V. (www.gauss-centre.eu) by providing computing time on the GCS Supercomputer SUPERMUC-NG at the Leibniz Supercomputing Centre (www.lrz.de). The CosmoSim data base (www.cosmosim.org) used in this paper is a service of the Leibniz Institute for Astrophysics Potsdam (AIP). Our collaboration has been supported by the DFG grant GO 563/24-1. This work has been partially supported by the Consejo de Investigaciones Científicas y Técnicas de la República Argentina (CONICET) and the Agencia Nacional de Promoción Científica y Tecnológica (PICT 2019–1600). NIL acknowledges financial support from the IDEXLYON Project at the University of Lyon under the Investments for the Future Program (ANR-16-IDEX-0005). NIL also acknowledge support from the joint Sino-German DFG research Project 'The Cosmic Web and its impact on galaxy formation and alignment' (DFG-LI 2015/5-1). SAC acknowledges funding from CONICET (PIP-2876), *Agencia Nacional de Promoción de la Investigación, el Desarrollo Tecnológico y la Innovación* (Agencia I+D + i, PICT-2018-3743), and the *Universidad Nacional de La Plata* (G11-150), Argentina. ANR acknowledges support from CONICET (PIP 11220200102832CO) and the Secretaría de Ciencia y Técnica de la Universidad Nacional de Córdoba (PID 33620180101077). CVM acknowledges support from ANID/FONDECYT through grant 3200918, and he also acknowledges support from the Max Planck Society through a Partner Group grant. GY acknowledges partial financial support from the Ministerio de Ciencia e Innovación (Spain) under research grant PID2021-122603NB-C21.

DATA AVAILABILITY

The data underlying this article will be shared on reasonable request to the corresponding author.

REFERENCES

Ahumada R. et al., 2020, ApJS, 249, 3
Aragón-Calvo M. A., van de Weygaert R., Jones B. J. T., van der Hulst J. M., 2007, ApJ, 655, L5
Behroozi P. S., Wechsler R. H., Wu H.-Y., 2013a, ApJ, 762, 109
Behroozi P. S., Wechsler R. H., Wu H.-Y., Busha M. T., Klypin A. A., Primack J. R., 2013b, ApJ, 763, 18
Blanton M. R., Eisenstein D., Hogg D. W., Schlegel D. J., Brinkmann J., 2005, ApJ, 629, 143
Boselli A., Cortese L., Boquien M., Boissier S., Catinella B., Lagos C., Saintonge A., 2014, A&A, 564, A66
Cora S. A. et al., 2018, MNRAS, 479, 2
de Jong R. S. et al., 2019, The Messenger, 175, 3
Delfino F. M., Scóccola C. G., Cora S. A., Vega-Martínez C. A., Gargiulo I. D., 2022, MNRAS, 510, 2900
DESI Collaboration et al.2016a, preprint (arXiv:1611.00036)
DESI Collaboration et al.2016b, preprint (arXiv:1611.00037)
Dressler A., 1980, ApJS, 42, 565
Duplancic F., Dávila-Kurbán F., Coldwell G. V., Alonso S., Galdeano D., 2020, MNRAS, 493, 1818
Gruppioni C. et al., 2015, MNRAS, 451, 3419
Hahn O., Carollo C. M., Porciani C., Dekel A., 2007b, MNRAS, 381, 41
Hahn O., Porciani C., Carollo C. M., Dekel A., 2007a, MNRAS, 375, 489
Henriques B. M. B., White S. D. M., Thomas P. A., Angulo R., Guo Q., Lemson G., Springel V., Overzier R., 2015, MNRAS, 451, 2663
Hoffman Y., Metuki O., Yepes G., Gottlöber S., Forero-Romero J. E., Libeskind N. I., Knebe A., 2012, MNRAS, 425, 2049
Huchra J. P., Geller M. J., 1982, ApJ, 257, 423
Ivezić Ž. et al., 2019, ApJ, 873, 111
Kauffmann G., White S. D. M., Heckman T. M., Ménard B., Brinchmann J., Charlot S., Tremonti C., Brinkmann J., 2004, MNRAS, 353, 713
Klypin A., Yepes G., Gottlöber S., Prada F., Heß S., 2016, MNRAS, 457, 4340
Knebe A. et al., 2018, MNRAS, 475, 2936
Kormendy J., Ho L. C., 2013, ARA&A, 51, 511
Libeskind N. I. et al., 2018, MNRAS, 473, 1195
Libeskind N. I., Hoffman Y., Forero-Romero J., Gottlöber S., Knebe A., Steinmetz M., Klypin A., 2013, MNRAS, 428, 2489
McConnell N. J., Ma C.-P., 2013, ApJ, 764, 184
Muratov A. L., Kereš D., Faucher-Giguère C.-A., Hopkins P. F., Quataert E., Murray N., 2015, MNRAS, 454, 2691
O'Mill A. L., Padilla N., García Lambas D., 2008, MNRAS, 389, 1763
Peng Y.-j. et al., 2010, ApJ, 721, 193
Planck Collaboration, XVI, 2014, A&A, 571, A16
Porciani C., Dekel A., Hoffman Y., 2002, MNRAS, 332, 339
Ruiz A. N. et al., 2015, ApJ, 801, 139
Ruiz A. N., Alfaro I. G., Garcia Lambas D., 2019, MNRAS, 483, 4070
Springel V., White S. D. M., Tormen G., Kauffmann G., 2001, MNRAS, 328, 726
Taverna A., Salerno J. M., Daza-Perilla I. V., Díaz-Giménez E., Zandivarez A., Martínez H. J., Ruiz A. N., 2023, MNRAS, 520, 6367
Tempel E., Tago E., Liivamägi L. J., 2012, A&A, 540, A106
Tully R. B. et al., 2006, AJ, 132, 729
Tully R. B., 1987, ApJ, 321, 280
Tully R. B., 1988, Science, 242, 310
Wang H. et al., 2018, ApJ, 852, 31
Wang P., Kang X., Libeskind N. I., Guo Q., Gottlöber S., Wang W., 2020, New A, 80, 101405
Wetzel A. R., Tinker J. L., Conroy C., 2012, MNRAS, 424, 232
Yang X., Mo H. J., van den Bosch F. C., Pasquali A., Li C., Barden M., 2007, ApJ, 671, 153
Yaryura C. Y. et al., 2020, MNRAS, 499, 5932

Zhang Y., Yang X., Faltenbacher A., Springel V., Lin W., Wang H., 2009, ApJ, 706, 747
Zheng Z. et al., 2017, MNRAS, 465, 4572

APPENDIX A: STABILITY OF CLASSIFICATION OF ENVIRONMENT

In this appendix, we analyse the robustness of our classification scheme of the large-scale matter distribution of the cosmic web according to the variation of the characteristic scale adopted to estimate the density of the environment. In particular, we evaluate how the number of associations categorized in a given environment (knot, filament, wall, or void) varies when changing the smoothing length ($l = 1$, 2, or 4 Mpc h^{-1}). These four categories are assigned according to the sign of the eigenvalues of the Hessian matrix estimated from the gravitational potential (see Section 4.1). To compute these eigenvalues, first, the full simulated box of the SMDPL simulation (described in Section 2.1) is covered with a fixed grid of 400^3 cells. Then, the DM particle overdensity is smoothed using a spherically symmetric Gaussian window function with a given l, and the gravitational potential is estimated. The gravitational potential (ϕ) is normalized by $4\pi G\overline{\rho}$, whereby it satisfies the Poisson equation ($\nabla^2\phi = \delta$), where δ is the dimensionless matter overdensity, G the gravitational constant, and $\overline{\rho}$ is the average density of the Universe. The Hessian matrix is constructed from this peculiar gravitational potential (tidal tensor), and we assign its three eigenvalues to each cell. Finally, we assign to each association the same eigenvalues as those of the cell in which the association centre is located. As expected, these eigenvalues depend on the l of the Gaussian filter. For a given l, the number of eigenvalues greater than a given threshold ($\lambda_{\rm th} = 0$) is used to classify the type of environment where each association resides: knot, filament, wall, or void. Table A1 presents the number of dwarf galaxy associations in each environment for the three different smoothing lengths.

Fig. A1 shows how systems are identified as part of one environment (knot, filament, wall, or void) or another according to the l used. The upper, middle, and lower panels show the comparison between $l = 1$ versus $l = 2$, $l = 1$ versus $l = 4$, $l = 2$ versus $l = 4$, and their reciprocals, respectively, as indicated by the legends. On the x-axis of each panel, there are four boxes corresponding to knots, filaments, walls, and voids. In each of the boxes, there are four bars with different colours identifying knots (black), filaments (blue), walls (magenta), and voids (green). The length of each bar corresponds to the ratio N_{XY}/N_Y, where N_{XY} is the number of objects belonging to category X in, for example, $l = 1$ but categorized as Y in, for example, $l = 2$, while N_Y is the total number of associations categorized as Y in $l = 2$ following the same example as above, where X and Y can take the values K, F, W, or V, for knot, filament, wall, and void, respectively. The mentioned example corresponds to $l = 1$ versus $l = 2$, shown in the upper-left panel of Fig. A1. Notice that,

Table A1. Number of dwarf galaxy associations in different environments (knots, filaments, walls, and voids) estimated from the tidal tensor for three different values of smoothing length, $l = 1$, 2, and 4 Mpc h^{-1}.

	Tidal		
	$l = 1$	$l = 2$	$l = 4$
Knots	17 671	28 087	34 667
Filaments	206 839	182 974	165 609
Walls	81 407	91 564	98 662
Voids	2333	5625	9312

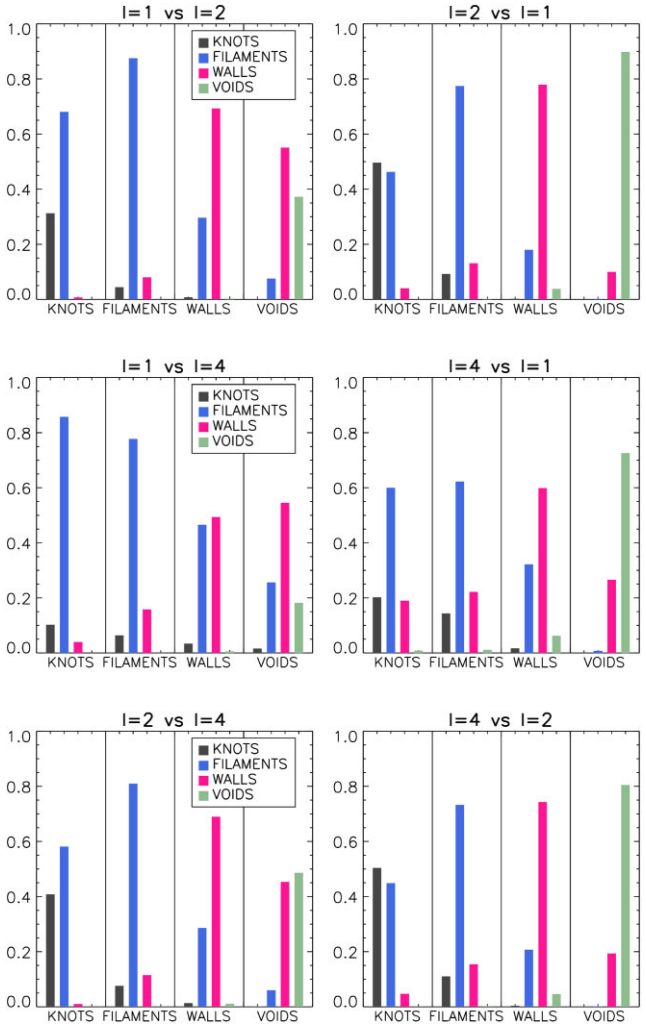

Figure A1. Change of associations from one category (knot, filament, wall, or void) to another according to the smoothing length used to estimate the eigenvalues, comparing two samples at a time. Upper, middle, and lower panels show the comparison between $l = 1$ versus $l = 2$, $l = 1$ versus $l = 4$, $l = 2$ versus $l = 4$, and their reciprocals, respectively, as indicated by legends.

with this definition, it is true that

$$N_Y = N_{\rm KY} + N_{\rm FY} + N_{\rm WY} + N_{\rm VY}, \quad \text{(A1)}$$

By definition, the sum of the length of the bars in each box is equal to 1, so the different lengths give an idea about the 'wandering' of objects from one environment to another of the cosmic web. If the bar length equals 1, all objects stay in the same environment. So, if the categorization does not change from one smoothing length to another, the first box of each panel (Y = K) should show only a black bar, the second box (Y = F) should show only a blue bar, the third box (Y = W) should show only a magenta bar, and the fourth box (Y = V) should show only a green bar, all of which should have the same length (equal to 1). Evidently, this is not what we see in Fig. A1. Filaments and walls seem to be the best defined environments. The classification of walls is a bit less stable, in particular, considering the large step from 1 to 4 Mpc h^{-1}. The right-hand panels show that decreasing the smoothing length keeps the objects in the same environment. The classification of filaments seems to be the most

stable, while the classification of knots is the most unstable for all cases.

Despite the variations described in the different categories when we classify the environment considering different smoothing length values, the results presented in this work are in full agreement for the three chosen smoothing lengths. Therefore, we decided to present only results based on the smoothing length 1 $\mathrm{Mpc\,h^{-1}}$. We have also tested the stability of the environment definition based on tidal tensor versus shear velocity. We find an 80–90 per cent agreement for filaments, walls, and voids. Again, the main results presented in this project are in full agreement if we use the shear velocity field instead of the tidal tensor.

This paper has been typeset from a TEX/LATEX file prepared by the author.